SSC08-VII-2

On-Orbit Spacecraft Inertia and Rate Sensor Scale Factor Estimation for Microsatellites

Philip A. Ferguson
Microsat Systems Canada Incorporated (MSCI)
3565 Nashua Drive, Mississauga, Ontario, Canada L4V 1R1; (905) 672-8828 ext. 237
pferguson@dynacon.ca

ABSTRACT

A key challenge in testing and operating small satellites is the determination of the moment of inertia. Attitude control systems engineers use the moment of inertia to develop closed loop pointing controllers as well as accurate feed-forward pointing commands that predict the satellite's motion. Traditionally, engineers measure the satellite moment of inertia using a mass properties table. However, for small, relatively lightweight satellites, this process is error-prone and costly regardless of the satellite size. This paper presents a novel on-orbit inertia-estimation technique. The algorithm is based on standard non-linear function solvers that can be run on the ground and requires only a rudimentary initial inertia estimate as a starting point (such an estimate can be obtained from structural modeling software). In addition to estimating the satellite inertia matrix, the estimator can also provide rate sensor scale-factor corrections. This paper demonstrates the inertia and scale factor estimator using the MOST spacecraft (now in its fifth year of operations).

MOTIVATION

Microsatellites have been identified as an enabling technology for science and defense[1,2]. With their small size and relatively low cost to build and launch, academia and industry alike are turning to small satellites to meet their mission[3,4]. As the popularity of microsatellites increases, so do the performance expectations of microsatellites. End users desire big-sat performance at the size and cost of a small-sat. To meet this goal, microsatellite prime contractors continually look for ways to improve pointing performance while reducing program costs.

One of the ways in which microsatellite prime contractors can reduce cost is to shorten the integration and test phase of the microsatellite program. This can be done by relying on engineering analysis and on-orbit commissioning to replace some of the ground testing that is typically part of big-satellite programs.

This paper specifically addresses mass properties testing. Typically, a fully-integrated spacecraft in its launch configuration is mounted to a mass properties table late in the integration and test program. The mass properties table spins the spacecraft about all three axes and measures the dynamic response to determine the full three-by-three inertia tensor as well as the location of the centre of mass.

The purpose of determining the mass properties is twofold. Firstly, launch providers impose inertia and centre of mass constraints on all payloads. As such, the launch providers typically require some evidence of testing or analysis to back up the mass properties estimates. Secondly, high performance attitude control systems use the inertia estimate of the satellite to compute accurate control torques aimed at providing fine pointing control.

An on-orbit method for precisely determining the inertia tensor could:

1. Eliminate or significantly reduce the scope of the mass properties testing required prior to launch (thus shortening the program schedule and reducing cost).

2. Increase the accuracy of the inertia estimate for control purposes since the spacecraft inertia would be evaluated while the spacecraft is in its deployed, on-orbit configuration as opposed to its launch configuration.

Case Study: Microvariability and Oscillations of Stars (MOST) Spacecraft

Recent analysis of slew performance on the MOST spacecraft (see Figure 1) has indicated that tracking errors due to feed-forward control commands may be due in part to errors in the pre-flight estimation of the spacecraft moment of inertia matrix (J). During integration and test activities, the MOST spacecraft underwent mass properties testing at the David Florida Laboratories (DFL) to determine its moment of inertia tensor and the location of the spacecraft centre of mass (see Figure 2). While the centre of mass location was only required for launch vehicle integration purposes,

the moment of inertia matrix plays a key role in the generation of feed-forward commands. As such, errors in J lead to feed-forward errors that must be corrected by the feedback control system.

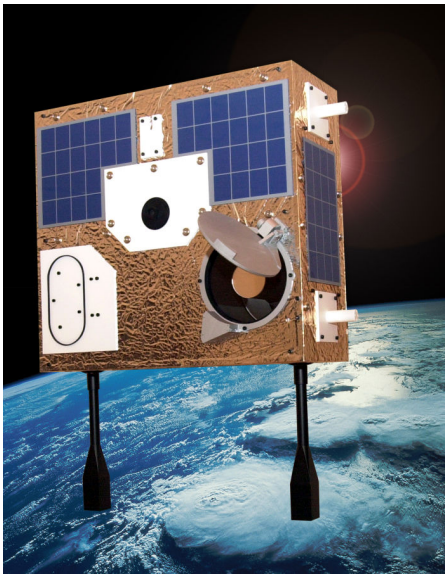

Figure 1: Artist's Concept of MOST On-Orbit

To correct these errors, a procedure was desired to obtain a more accurate estimate of J while the spacecraft is on-orbit. By applying known torques to the spacecraft using the on-board reaction wheels and monitoring the resulting motion, a non-linear estimator was developed to compute the elements of the J matrix.

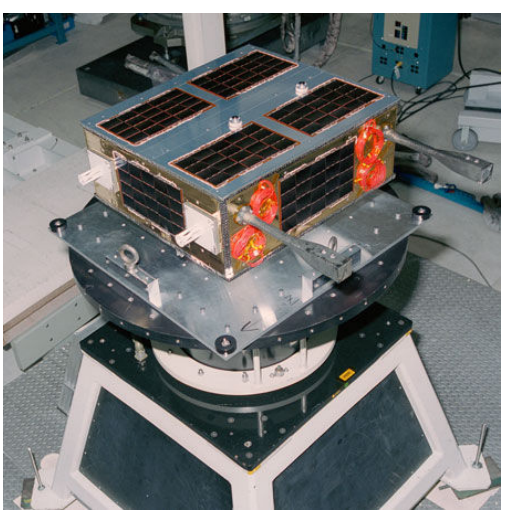

Figure 2: MOST Spacecraft during Mass Properties Testing

ON-ORBIT INERTIA ESTIMATION

Developing an on-orbit inertia estimator requires careful consideration of the dynamics, available sensor observations and the resulting observability of the spacecraft system. In the absence of perfect measurements, imperfect sensors must be used to estimate the inertia tensor.

Dynamics

The familiar rotational dynamics of a rigid body are:

$$\tau_d = \dot{h} \tag{1}$$

where τ_d is the external disturbance torque on the spacecraft, h is the total spacecraft momentum and the dot denotes time differentiation. The momentum of a rigid body spinning at a rate of ω is:

$$h_{body} = J\omega \tag{2}$$

If reaction wheels are used, the stored reaction wheel momenta (h_w) contribute to the total spacecraft momentum as:

$$h = h_{body} + h_w = J\omega + h_w \tag{3}$$

Substituting Equation (3) into Equation (1):

$$\tau_d = J\dot{\omega} + \omega^{\times} J\omega + \omega^{\times} h_w + \dot{h}_w \tag{4}$$

Usually, the $\dot{h}_w$ term is written as a control torque as:

$$\tau_c = -\dot{h}_w \tag{5}$$

Finally, Equation (4) can be rewritten as:

$$\tau_c + \tau_d = J\dot{\omega} + \omega^{\times} J\omega + \omega^{\times} h_w \tag{6}$$

Equation (6) illustrates the non-linear relationship between the inertia tensor (J) and the body rates.

By integrating Equation (6), a time history of body rates can be computed. From the time history of body rates, the orientation of the spacecraft can be obtained in a using a quaternion formulation. The quaternion is defined as[5]:

$$q = \begin{bmatrix} \varepsilon \\ \eta \end{bmatrix} \tag{7}$$

where

$$\varepsilon = a\sin\left[\frac{\phi}{2}\right] \tag{8}$$

$$\eta = \cos\left[\frac{\phi}{2}\right] \tag{9}$$

and the variables a and ϕ represent the Euler axis and angle parameters respectively. With a time history of body rates, the quaternion dynamics are defined by the following equations:

$$\dot{\varepsilon} = \frac{1}{2}\left(\varepsilon^{\times} + \eta\mathbf{1}\right)\omega \tag{10}$$

$$\dot{\eta} = -\frac{1}{2}\varepsilon^{T}\omega \tag{11}$$

By integrating the above equations, a time history of quaternions can be computed. The next section describes the measurements assumed to be available for estimating the inertia tensor.

Measurements

Most inertial-pointing microsatellites require rate sensors to support slew control. A cluster of rate sensors can provide three-axis spin rate information, depending on their configuration. However, all rate sensors suffer from the following shortcomings:

1. Temperature-dependent bias error
2. Scale factor error

Equation (7) illustrates how the rate sensor bias and scale factor errors affect the rate sensor measurements:

$$K\omega_{meas} = C_{rate}\omega_{true} + b \tag{12}$$

where ω_{true} is the vector of the actual spacecraft body rates, ω_{meas} is the vector of the rate sensor measurements, K is a diagonal matrix containing the rate sensor scale factors (one for each rate sensor) b is the vector of the rate sensor biases (one for each rate sensor) and C_{rate} is the transformation matrix used to express body rates in the local sensor frame.

On most spacecraft, the rate sensor biases are usually estimated and compensated for by the attitude estimator[6]. This estimation technique uses information from other absolute position sensors to derive the bias for each rate sensor. As such, rate sensor bias errors would not affect inertia estimation.

The rate sensor scale factor errors can be partially temperature dependent, but generally arise from mounting misalignments and small errors during calibration. If rate sensors are to be used as inputs to an inertia estimation routine, the rate sensor scale factor errors must be accounted for to prevent erroneous inertia estimates.

In much the same way that the rate sensor biases can be estimated using other absolute position sensors, so too can the rate sensor scale factors. A star tracker can provide a highly-accurate attitude measurement (in the form of a quaternion) to complement the rate sensor measurements. The following subsection describes the theory behind a combined inertia and rate sensor scale factor estimator using rate sensor and star tracker measurements.

Estimator Design

Since the inertia tensor is a dynamic quantity, spacecraft rotational motion is required to fully observe its components. The estimation process involves commanding a series of slews that adequately exercise rotational motion about all three orthogonal axes of the spacecraft. Rate sensor measurements are collected throughout each slew as well as star tracker measurements immediately prior to and following each slew. Note that relatively fast slews (on the order of one degree per second) are required such that the off-axis gyric motion of the satellite (which defines off-axis terms of the inertia estimator) can be observed using the rate sensors. The required slew rates depend on the accuracy of the rate sensors. Larger slew rates produce larger gyric precessions which must be large enough to be measured by the rate sensors at an acceptable signal to noise ratio. At such large slew rates, it is assumed that star tracker measurements during the slew are not available (and only available immediately prior to and following the slew).

The inertia and rate sensor scale factor estimator design is based on the fundamental principle behind all estimators: to determine the state vector that minimizes the difference between the actual measurements and the computed measurements based on the state vector.

The above statement can be stated mathematically as: Find the state vector, $\hat{X}$, that minimizes the cost functional:

$$\Theta = \left(y - z\left(\hat{X}\right)\right)^{T} R^{-1}\left(y - z\left(\hat{X}\right)\right) \tag{13}$$

Where y is the vector of measurements, $z\left(\hat{X}\right)$ is the vector of computed measurements using the state vector $\hat{X}$ and R^{-1} is the measurement noise matrix that weights measurements differently based on their relative sensor noise. The case where a linear relationship exists between the measurements and the state vector as:

$$z\left(\hat{X}\right) = H\hat{X} \tag{14}$$

And where the measurements are tainted with purely Gaussian noise, has a well-documented solution known as the weighted least squares estimator (WLSE)[7]. In this case, the optimal solution takes the form:

$$\hat{X} = \left(H^T R^{-1} H\right)^{-1} H^T R^{-1} y \tag{15}$$

A non-linear version of the WLSE[8], however it requires explicit computation of $\frac{\partial z\left(\hat{X}\right)}{\partial \hat{X}}$. In the case of the inertia estimator with three rate sensors, the state vector is:

$$\hat{X} = \begin{bmatrix} J_{xx} \\ J_{yy} \\ J_{zz} \\ J_{xy} \\ J_{xz} \\ J_{yz} \\ K \end{bmatrix} \tag{16}$$

where

$$J = \begin{bmatrix} J_{xx} & J_{xy} & J_{xz} \\ J_{xy} & J_{yy} & J_{yz} \\ J_{xz} & J_{yz} & J_{zz} \end{bmatrix} \tag{17}$$

is the full 9x9 symmetric inertia tensor and

$$K = \begin{bmatrix} K_1 \\ K_2 \\ K_3 \end{bmatrix} \tag{18}$$

is the vector of rate sensor scale factors (in this case, assuming three rate sensors are present. Note that the nonlinear dynamics of Equations (6), (10) and (11) do not lend themselves easily to isolating the measurement vector as a function of the state vector or the required partial derivative. As such, a different method of estimating the inertia tensor and rate sensor scale factors was required. However, while the closed form solutions of the WLSE and the non-linear WLSE are not applicable to the inertia estimation problem, the fundamental principle of finding the state vector that minimizes the difference between the actual and computed measurements still holds.

By assuming a particular inertia tensor and set of rate sensor scale factors, the cost functional can be computed for each slew using the commanded torques, measured wheel momenta and non-linear dynamics of Equations (6), (10) and (11). Figure 3 illustrates how the cost is computed for a single slew based on a particular estimate of J and K:

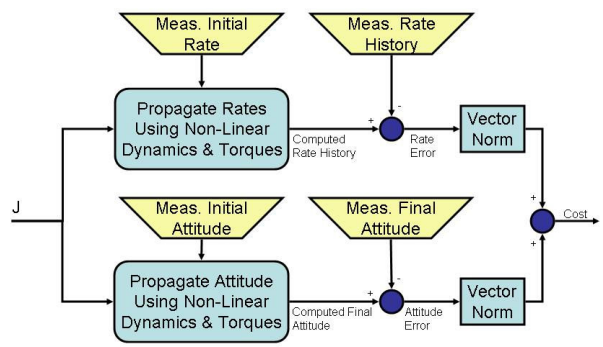

Figure 3: Cost Computation Algorithm per Slew

Figure 4 illustrates how the costs from each test slew are combined to form a total cost that can be minimized though the selection of appropriate values of J and K.

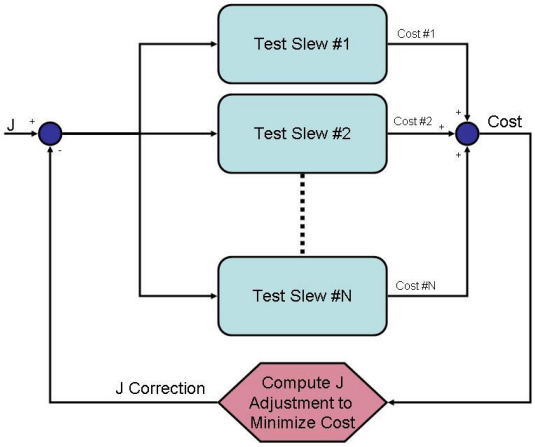

Figure 4: Optimization Algorithm

The function minimization can be carried out using any non-linear function solver. For the results presented in this paper, the author used the Matlab™ function: `fmincon.m` to minimize the cost functional, however many other function-minimizing techniques are available[9].

RESULTS

This section provides results from a simulation of MOST and from actual MOST flight data that demonstrate the effectiveness of the inertia and rate sensor scale factor estimator presented in this paper.

Simulations

As part of MOST operations, MSCI maintains a dynamic simulator of the MOST microsatellite. The simulator enables the user to define a true inertia (used in the dynamics engine of the simulator) different from the control inertia (used by the attitude controller). Similarly, the user can inject incorrect rate sensor scale factors.

With errors ranging from one to four percent on all components of the inertia tensor and all three rate sensor scale factors, a set of five slews were conducted to produce body rates about all three axes. Figure 5 illustrates the slew profiles of each test slew used in the simulator.

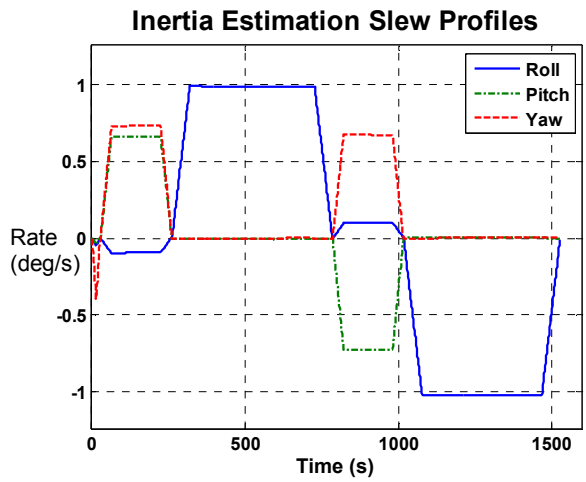

Figure 5: Test Slew Profiles for Simulated Inertia Estimation

Table 1 summarizes the results of the simulated inertia estimation procedure (all inertias are reported in units of kg-m^2).

Table 1: Simulated Inertia Estimation Results

	True Value	Initial Est.	Initial Error	New Est.	New Error
J_{xx}	3.3311	3.3977	-2%	3.3461	-0.45%
J_{yy}	2.2024	2.1363	3%	2.2060	-0.16%
J_{zz}	1.8033	1.8394	-2%	1.7965	0.37%
J_{xy}	-0.0119	-0.0124	-4%	-0.0023	81.0%
J_{xz}	0.0027	0.0028	-3%	0.0017	37.8%
J_{yz}	0.0161	0.0158	2%	0.0222	-37.7%
K_1	1.01	1.00	-1%	1.0099	0.01%
K_2	1.02	1.00	-2%	1.0228	-0.28%
K_3	0.98	1.00	2%	0.9792	0.08%

The results in Table 1 show a dramatic error reduction in the primary components of the inertia tensor as well as the three rate sensor scale factors. While the cross terms in the inertia tensor get worse following the estimation procedure, their magnitude with respect to the diagonal entries indicates suggests they play a minor role in the dynamics.

Table 2 demonstrates the overall performance increase resulting from the inertia estimation procedure. The MOST slew control strategy first performs a fast (one degree per second) slew, followed by a fine correction slew. The fast slew uses rate sensors alone since the star tracker is not sensitive enough for stars streaking across the CCD at one degree per second. The purpose of the fine correction slew is thus to correct for errors resulting from feedforward control errors (*i.e.,* inertia errors) and rate sensor errors (*i.e.,* rate sensor bias drift and rate sensor scale factor errors). As such, the size of the correction slew is a good indicator of the quality of the inertia estimate as well as the rate sensor scale factors (in addition to the rate sensor bias drift during the slew since bias estimation is typically not done during slews).

Table 2: Simulated Performance Improvements

	Old Params	New Params
Correction Slew Size (arcseconds)	349	140

The data in Table 2 indicates that the size of the simulated correction slew reduced by more than a factor of two following a slew of approximately five degrees.

MOST Data

Prior to launch, MOST underwent mass properties testing at the David Florida Laboratories (DFL) in Ottawa, Ontario, Canada. At that time, the inertia tensor was measured and uploaded into the spacecraft software.

In July, 2007, a set of five inertia estimation slews were commanded on the MOST spacecraft. Figure 6 illustrates the slew profiles commanded on the MOST spacecraft for the purpose of inertia estimation.

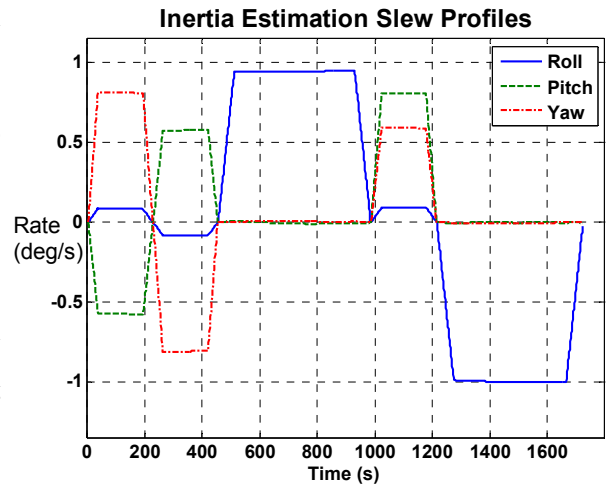

Figure 6: Test Slew Profiles for MOST Inertia Estimation

Table 3 summarizes the results of the MOST inertia estimation procedure (all inertias are reported in units of kg-m^2). Of course, a true measure of the MOST inertia is not available.

Table 3: MOST Inertia Estimation Results

	Initial Est.	New Est.
J_{xx}	3.4084	3.3853
J_{yy}	2.1836	2.2168
J_{zz}	1.6808	1.7868
J_{xy}	-0.0407	-0.0273
J_{xz}	-0.0958	-0.0033
J_{yz}	0.0208	0.0052
K_1	1.0000	1.0072
K_2	1.0000	1.0028
K_3	1.0000	1.0037

To evaluate the quality of the inertia tensor and rate sensor scale factor estimates, identical slews prior to and following the inertia estimation procedure were compared. Table 4 illustrates the reduction in size of the correction slew following a 38-degree slew command.

Table 4: MOST Performance Improvements

	Old Params	New Params
Correction Slew Size (arcseconds)	1641	1020

The data in Table 4 indicates that a 38% reduction in the size of the correction slew occurred resulting from the inertia and rate sensor scale factor updates. As such, the update was deemed effective and worthwhile.

DISCUSSION

It should be noted at this point that errors in the moment of inertia tensor are not the only errors that cause feed-forward control errors. Other possible sources of error include:

- Misalignment errors
  - Reaction wheel / star tracker misalignment
  - Reaction wheel / rate sensor misalignment
  - Rate sensor / star tracker misalignment
- Reaction wheel torque application errors
- Reaction wheel command lag
- Rate sensor bias errors
- Disturbance torques

While the above errors are important, they have either not been considered or compensated for during the inertia estimation. The following subsections describe how each type of error was treated during the inertia estimation:

Misalignment Errors

Misalignment errors have the potential to produce large pointing errors during slews, depending on the size of the slew. For the rate sensors, the magnitude of the error varies as the sine of the slew angle. As such, rate sensor misalignments have no effect for slews of 180 degrees and their maximum is for slews of 90 degrees. In order to minimize the effect of misalignment errors on the inertia estimation, slews close to 0 or 180 degrees should be planned during the inertia estimation procedure.

While it may be possible to design test slews that are either very small or very large (*i.e.,* close to 180 degrees), viewing zone limitations may make this constraint impractical to meet. However, since the inertia estimator presented herein also estimates the rate sensor scale factors, it is possible that rate sensor and reaction wheel misalignments could be partially compensated for by modified rate sensor scale factors. This is because, to first order, misalignment errors tend to manifest themselves as slight insensitivities to on-axis motion.

Reaction Wheel Torque Application Errors

In many cases, a torque application error is indistinguishable from an inertia error about the wheel axis. From the inertia estimator's perspective, all torque application errors will be interpreted as inertia errors. As such, reaction wheel torque errors will be compensated by adjusting the inertia tensor. As is the case with the misalignment errors, a purposefully "incorrect" inertia tensor and/or rate sensor scale factors can compensate for wheel torque application errors.

If torque application and/or misalignment errors are suspected, extra care should be taken when using the modified inertia tensor and rate sensor scale factors. If a different combination of reaction wheels and rate sensors were to be used (*e.g.,* switching to a backup reaction wheel or sensor), the inertia estimation would need to be repeated since torque application errors and misalignments are specific to particular sensors and actuators, rather than the inertia which has been modified.

Reaction Wheel Command Lag

Reaction wheel command lag can be compensated for, as long as the lag is well-known. Prior to executing the inertia estimation procedure, this lag would need to be identified and incorporated into the dynamics to ensure that command lags are not interpreted as inertia errors.

Rate Sensor Bias Errors

During normal operations, the Extended Kalman Filter (EKF) estimates the rate sensor biases. To remove complexity from the inertia estimator, the rate sensor biases are not included in the filter. Prior to estimating the inertia matrix, a snapshot of the current rate sensor biases should be taken. These biases should then be used during the inertia estimation process to correct the rate sensor measurements. Assuming that the biases will not change appreciably during the short inertia

identification process, this approximation should not result in large inertia estimation errors.

Disturbance Torques

Disturbance torques will be present during the inertia estimation and will taint the estimates. The most prominent disturbance torque will be due to magnetic dipoles in the spacecraft interacting with the earth's magnetic field. Magnetic torques of this nature are periodic with a period of a half orbit (or approximately 50 minutes at the altitude of MOST). To minimize the effect of the disturbance torques, the time required to perform the estimation process should be minimized.

CONCLUSIONS

This paper has presented a unique technique for estimating the inertia tensor. To ensure accurate estimation results, the rate sensor scale factors are also estimated along with the inertia tensor.

Results from both the MOST simulator and the actual MOST spacecraft on-orbit indicate that the inertia estimation technique is not only effective but worthwhile since better inertia estimates reduce the size of correction slews required.

While launch providers will likely continue to require explicit mass properties testing, the techniques presented in this paper enable a spacecraft controls engineer to further hone the inertia estimates during spacecraft commissioning. On-orbit inertia estimation also ensures that the spacecraft is being evaluated in its on-orbit / operational configuration, which may not be possible on the ground prior to launch.

While such a procedure has proven effective at improving the performance of MOST, it provides much more benefit to future microsatellites such as NEOSSat (Near Earth Object Surveillance Satellite). With a procedure and associated analysis algorithms available to identify the spacecraft inertia matrix on-orbit, it may be possible to eliminate or significantly reduce the scope of the inertia identification element of the mass properties testing activities. A rudimentary inertia estimate could be obtained from the structural analysis software prior to launch. This inertia matrix could be used until a more accurate inertia matrix could be obtained during the on-orbit identification procedure outlined in this document.

ACKNOWLEDGEMENTS

The author of this paper would like to thank his colleagues at MSCI, Inc and chief operators of the MOST microsatellite, Jamie Wells and Ron Wessels for arranging and running the slews required to test this inertia estimation technique. In addition, the author would like to thank Professor Jamie Matthews, the principal investigator behind the MOST microsatellite, from the University of British Columbia and the Canadian Space Agency for generously donating two orbits of time on the MOST microsatellite in which to run these inertia estimation tests.

Finally, the author would also like to thank David Cooper, the president and CEO of MSCI for continually fostering a work environment that encourages research endeavours such as the one presented in this paper.

References

1. Scott, L. et al., "Microsatellites Show Technical Promise for Space Surveillance," CASI ASTRO 2006, 25-27 April 2006.
2. Bedard, D. and Spaans, A., "Responsive Space for the Canadian Forces," 5th Responsive Space Conference, Los Angeles, CA, April 2007. RS5-2007-3004.
3. Grocott, S. C. O., Zee, R. E., Wells, G. J., Wessels, R., Beattie, A. and Park, S., "Expanding Capabilities of the MOST Spacecraft,", CASI ASTRO 2006, Montreal, April 2006.
4. Hildebrand, A. R., Cardinal, R. D., Carroll, K. A., Faber, D. R., Tedesco, E. F., Matthews, J. M., Kuschnig, R., Walker, G. A. H., Gladman, B., Pazder, J., Brown, P. G., Larson, S. M., Worden, S. P., Wallace, B. J., Chodas, P. W., Muinonen, K. and Cheng, A., "Modern Meteor Science: An Interdisciplinary View. Chapter 5: Advantages of Searching for Asteroids from Low Earth Orbit: The NEOSSat Mission, Springer Netherlands, 2005.
5. Hughes, P. C., Spacecraft Attitude Dynamics, Dover Publications, Mineola, New York, 1986.
6. Lefferts, E. J., Markley, F. L. and Shuster, M. D., "Kalman Filtering for Spacecraft Attitude Estimation", Journal of Guidance, Control and Dynamics, Vol. 5, No. 5, September–October 1982, pp. 417–429.
7. Gelb, A., Applied Optimal Estimation, The Analytic Sciences Corporation, Massachusetts Institute of Technology, Cambridge, Massachusetts, 1974.
8. Maybeck, P., Stochastic Models, Estimation, and Control, Academic Press, 1982.
9. Press, W. H., Teukolsky, S. A., Vetterling, W. T. and Flannery, B. P., Numerical Recipes 3rd Edition: The Art of Scientific Computing, Cambridge University Press, 2007.